

# Effective stabilization of photobleaching of BAC-Si in bismuth- and erbium-codoped optical fibers by 830 nm laser repeated pumping

Qi Yang (杨琪)<sup>1,2</sup>, Boyang Hu (胡博洋)<sup>3</sup>, Jie Gao (高洁)<sup>3</sup>, Hongxin Ding (丁鸿鑫)<sup>3</sup>, Jialang Huang (黄佳浪)<sup>3</sup>, Yushi Chu (楚玉石)<sup>1,2,3\*</sup>, Jianzhong Zhang (张建中)<sup>1,2\*\*</sup>, and Gang-Ding Peng (彭纲定)<sup>4</sup>

<sup>1</sup>Key Laboratory of In-fiber Integrated Optics of Ministry of Education, College of Physics and Optoelectronic Engineering, Harbin Engineering University, Harbin 150001, China

<sup>2</sup>Key Laboratory of Photonic Materials and Devices Physics for Oceanic Applications, Ministry of Industry and Information Technology, College of Physics and Optoelectronic Engineering, Harbin Engineering University, Harbin 150001, China

<sup>3</sup>Fiber Optical Sensing Center for Excellence, Yantai Research Institute, Harbin Engineering University, Yantai 264006, China

<sup>4</sup>Photonics and Optical Communications, School of Electrical Engineering and Telecommunications, University of New South Wales, Sydney NSW 2052, Australia

\*Corresponding author: [chuyushi@hrbeu.edu.cn](mailto:chuyushi@hrbeu.edu.cn)

\*\*Corresponding author: [zhangjianzhong@hrbeu.edu.cn](mailto:zhangjianzhong@hrbeu.edu.cn)

Received May 13, 2024 | Accepted July 23, 2024 | Posted Online February 10, 2025

The photobleaching (PB) effect of bismuth active center (BAC)-related silicon (BAC-Si) in the bismuth- and erbium-codoped optical fiber (BEDF) under repeated pumping was studied. The results demonstrated that the irreversible PB could be eliminated after repeated pumping, while the rest of the PB could be decreased and remained stable in the subsequent pumping. The mechanism was also discussed using electron transferring theory and the distribution function concept of activation energy. Moreover, the results also demonstrated that BAC-Si could further become stable, reversible, and irreversible after PB, and new standards can be established for the BEDF to evaluate its quality.

**Keywords:** bismuth- and erbium-codoped optical fiber; photobleaching; fiber laser; fiber amplifier.

DOI: [10.3788/COL202523.010604](https://doi.org/10.3788/COL202523.010604)

## 1. Introduction

To meet the requirements of large-capacity data transmission, the first report of ultrabroadband near-infrared (NIR) luminescence of bismuth-doped silica glass<sup>[1]</sup> has led to extensive research and remarkable developments in the field of bismuth-doped NIR luminescence materials and properties<sup>[2–8]</sup>. In 2005, Dianov *et al.* reported the bismuth-doped aluminosilicate glass fiber (BDF) fabricated by modified chemical vapor deposition (MCVD) technology and obtained a continuous laser emission in the spectral range of 1150–1300 nm<sup>[9]</sup>. In 2012, Peng *et al.* expanded the emission bandwidth by co-doping bismuth and erbium and obtained a codoped optical fiber (BEDF) using MCVD and *in situ* solution doping technologies, and an ultrabroad emission band covering the O-L band was realized under a single wavelength excitation<sup>[10,11]</sup>. The ultrabroadband NIR emission of the BDF is contributed by several BACs, such as BAC-related aluminum, phosphorus, silicon, and germanium, denoted as BAC-Al, BAC-P, BAC-Si, and BAC-Ge, respectively<sup>[12,13]</sup>.

Although BDFs have excellent NIR luminescence, the origin of BACs is still unclear because BACs are sensitive to glass composition and fabrication processes. Various posttreatments on BDFs are beneficial to understanding the nature of BACs, such as thermal and photo irradiation<sup>[14–17]</sup>. The emission intensities of BACs generally change after these treatments. Specially, when the BDFs are under laser irradiation, the bismuth active centers are likely to be destroyed, converting to inactive bismuth centers. The result of this process is manifested as the reduction of BAC-related absorption and luminescence. This phenomenon is called the photobleaching (PB) effect, which limits the potential of BDFs to become the gain material for ultrabroadband fiber amplifiers or tunable fiber lasers. For instance, in the case of the BAC-Si in the BEDF, the luminescence and resonant absorption were bleached partially under 1 h of 830 nm laser pumping; the bleached part fully recovered 48 h after the pump had stopped<sup>[18]</sup>. When the BEDF was pumped by the 830 nm laser for 9 h, the luminescence of BAC-Si was bleached by 34.5% but recovered only by 6.4% 91 h after the pump had

stopped<sup>[19]</sup>, which was different from the study above<sup>[18]</sup>. It can be inferred from the above that the deactivated BAC-Si can recover and convert to the active BAC-Si when the 830 nm laser is off. For simplicity, we refer to this process as recovery relaxation. In order to illustrate the influence of recovery relaxation on the PB effect in the BEDF, in this Letter, we observed and discussed the PB of BAC-Si in the BEDF under repeated 830 nm laser pumping, which was different from single continuous 830 nm laser pumping.

## 2. Experiments and Setup

The BEDF sample was fabricated by MCVD and *in situ* solution doping technologies. The core composition is SiO<sub>2</sub> ~ 85, GeO<sub>2</sub> ~ 12.9, P<sub>2</sub>O<sub>5</sub> ~ 0.94, Al<sub>2</sub>O<sub>3</sub> ~ 0.15, Er<sub>2</sub>O<sub>3</sub> ~ 0.01, and Bi<sub>2</sub>O<sub>3</sub> ~ 0.16 in mole fraction. The sample of BEDF has a numerical aperture (NA) of ~0.19, a core diameter of 4.8 μm, and a cutoff wavelength of ~1.68 μm. The inset of Fig. 1 is the photograph of the cross section of BEDF under a metallographic microscope (Axioscope 5, Zeiss). Figure 1 demonstrates the loss spectrum (red solid line) of BEDF in the range of 750–1650 nm and the emission spectrum (blue solid line) under 830 nm excitation. The loss spectrum was measured by the insertion loss method. Six absorption peaks were observed:

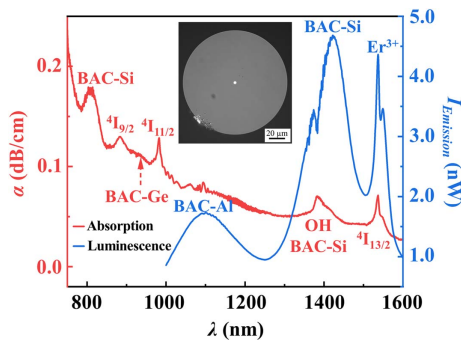


Fig. 1. Loss (red line) and emission (blue line) spectra of the pristine FUT; inset, cross section photo of the FUT.

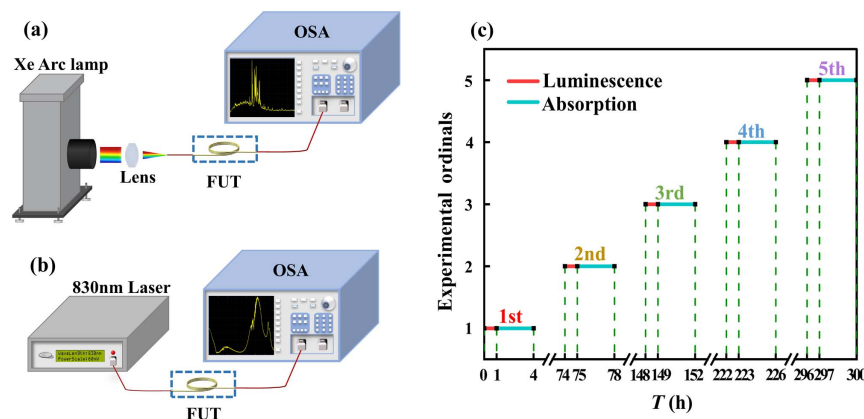


Fig. 2. Experimental setup of (a) loss and (b) emission measurements; (c) experimental process of repeated pumping.

808 nm for BAC-Si; 1384 nm for the overlapping absorption of BAC-Si and OH overtones; 935 nm for BAC-Ge; 883, 982, and 1536 nm for the electronic transitions of Er ions corresponding to  $^4I_{15/2} \rightarrow ^4I_{9/2}$ ,  $^4I_{15/2} \rightarrow ^4I_{11/2}$ , and  $^4I_{15/2} \rightarrow ^4I_{13/2}$ , respectively. Three luminescence peaks were observed at 1100 nm for BAC-Al, 1424 nm for BAC-Si, and 1536 nm for Er<sup>3+</sup><sup>[10,20]</sup>.

The experimental configuration is shown in Fig. 2. The fiber under test (FUT) is a section of BEDF (100 cm). Figure 2(a) shows the insertion loss method to obtain the absorption of BACs. An Xe arc lamp (6280NS, Newport) was selected as the white-light source. The white light was launched into the fiber through a 40× microscope objective, then recorded by an optical spectrum analyzer (OSA: AQ6374, Yokogawa) without or with the FUT. The FUT was pumped repeatedly by the 830 nm laser 5 times, and the pumping duration time was 1 h each time. The interval between pumping was around 73 h to ensure that the FUT had sufficient relaxation time after pumping. In order to evaluate the PB effect in the BEDF, an 830 nm continuous-wave (CW) fiber laser (COSC-830-80) was used as the pump source, and the changes of forward emission spectra of the FUT were recorded by the OSA, presented in Fig. 2(b). The experimental operation process of repeated pumping is depicted in Fig. 2(c). In each pumping process, the emission spectra of the FUT were recorded every 1 min in the first 20 min, and then recorded every 2–5 min in the second 20 min and the last 20 min, respectively. During the whole experiment, the output power of the 830 nm fiber laser was fixed to 60 mW to ensure that the input power to the FUT was consistent in each pumping. The transmission spectra of the white-light source from the pristine FUT and 5 min and 1, 3, and 73 h after the pump was off were recorded, respectively.

## 3. Results and Discussion

The emission spectra of the FUT of the first pumping process are shown in Fig. 3(a). The emission peaks of BAC-Al, BAC-Si, and Er<sup>3+</sup> were clearly identified. However, the changing trend of emission intensities was different; compared with other emission peaks, the emission intensity of BAC-Si obviously decreased

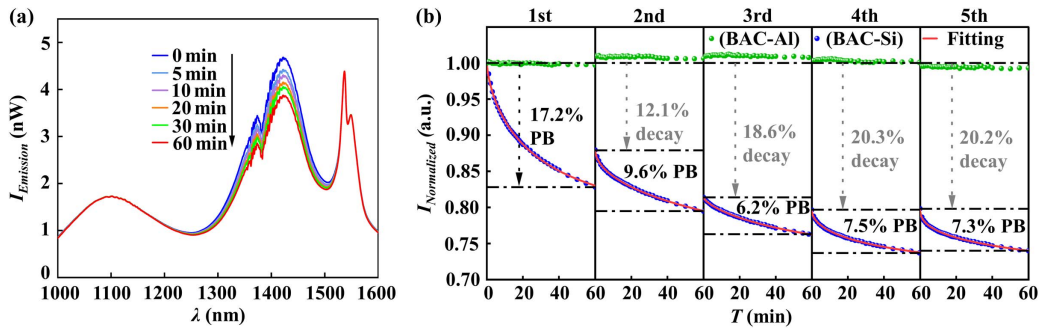


Fig. 3. (a) Emission spectra of the FUT under 830 nm excitation at 0, 5, 10, 20, 30, and 60 min during the first pumping process; (b) normalized luminescence intensities of BAC-Si (blue points) and BAC-Al (green points), and SEF fitting curve (red solid lines) with pumping time.

with pumping time. Figure 3(b) summarizes the normalized luminescence decay of BAC-Si at 1424 nm with the pumping time and fitted with the stretched exponential function (SEF), describing the relaxation of charge from a glass. In order to quantitatively describe the PB effect of BAC-Si in the FUT, we normalized the luminescence (the luminescence measured at the initial pumping time is the initial value) and expressed the SEF as

$$I(t) = I_{A,\infty} + (1 - I_{A,\infty}) \times \exp(-(t/\tau)^\beta), \quad (1)$$

where  $I(t)$  is the normalized luminescence intensity of BAC-Si at  $t$ ,  $I_{A,\infty}$  is the luminescence intensity when the PB is saturated,  $\tau$  is the time constant representing the speed of PB, and  $\beta$  is the stretched parameter. The green measured points show the variation of the luminescence intensity of BAC-Al at 1100 nm. The results show that the luminescence of BAC-Al remained stable and had only slight fluctuations during 830 nm pumping. The BAC-Al had no PB under repeated pumping. The blue measured points represent the luminescence change of BAC-Si at 1424 nm. It can be seen that in five experiments, with the increase in pumping time, the luminescence of BAC-Si showed a decaying trend. In the first 10 min after the pump was on, the luminescence decayed rapidly, and then gradually slowed down and eventually flattened out. In the first experiment, after 1 h of

pumping, the luminescence of BAC-Si decayed by about 17.2%. In the second, third, fourth, and fifth experiments, the attenuation was about 9.6%, 6.2%, 7.5%, and 7.3% respectively. The red solid lines are the results of the SEF fitting shown in Fig. 3(b). We can see that the SEF described the luminescence decay of BAC-Si in the FUT with pumping time well ( $R$ -square > 0.999). The results of the repeated pumping experiment indicated that the PB effect in the FUT was gradually weakened and tended to be stable in the subsequent repeated pumping.

The change of the insertion loss of the FUT was recorded during the recovery relaxation process for five experiments, as shown in Fig. 4. We first recorded the transmission spectrum of the white-light source without the FUT, and then recorded the transmission spectra through the pristine FUT and at 5 min and 1, 3, and 73 h after the pump was off in every experiment. The insertion loss was calculated by

$$\alpha = 10 \times \lg\left(\frac{T_{WL}}{T_{FUT}}\right)/L(\text{dB/cm}), \quad (2)$$

where  $T_{WL}$  is the transmission spectrum of white light without the FUT in loss measurement configuration,  $T_{FUT}$  is the transmission spectrum of white light with the FUT in configuration, and  $L$  is the length of the FUT. The loss spectrum of the pristine

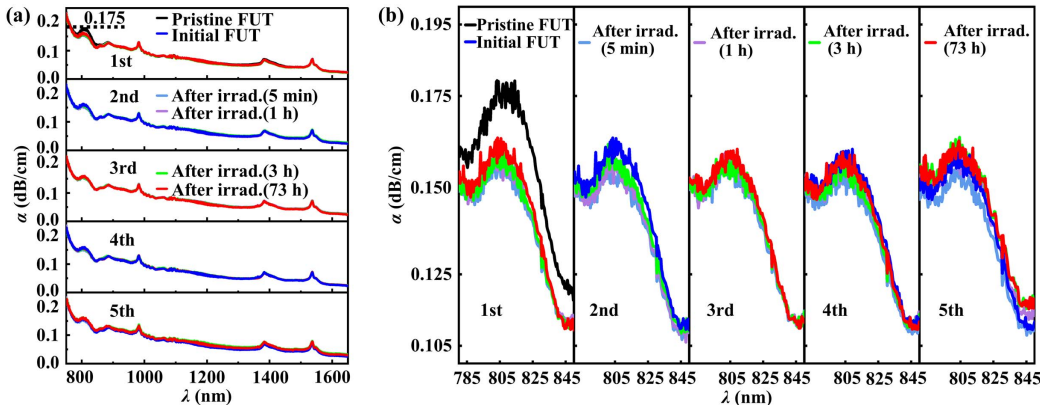


Fig. 4. (a) The change of insertion loss of the FUT during the recovery relaxation after the pump is off for five experiments; (b) enlarged parts of the band from 780 to 850 nm. irrads., irradiation.

FUT that has not been repeatedly pumped is shown by the black solid line. We considered the loss spectrum of 73 h after the pump was off as the initial loss spectrum (dark blue solid line) before the next pump started. The loss peak at 808 nm of the pristine fiber obviously reduced after 1 h of pumping, but there was only a slight recovery 73 h after the pump was off, while other loss peaks had no noticeable change. The band from 780 to 850 nm in Fig. 4(a) was enlarged and shown in Fig. 4(b) to depict the change of loss of BAC-Si more clearly. The loss of the pristine FUT was 0.175 dB/cm and reduced to 0.155 dB/cm 5 min after the pump was off and recovered to 0.160 dB/cm 73 h after the pump was off in the first experiment. In the subsequent pumping experiments, the loss was first reduced and then was partially restored. The loss at 1424 nm only had a slightly obvious change in the first experiment; the change in loss at 1424 nm in the subsequent experiment was too small to account for the change of BAC-Si. The change of loss insertion of the FUT during the recovery relaxation corresponded to the change of luminescence of BAC-Si, i.e., the luminescence intensity of BAC-Si decayed significantly during pumping but recovered partially during the recovery relaxation process. It should be noted that there was no insertion loss at 73 h after the pump was off in the second experiment because the Xe arc lamp did not run normally because the environment humidity was above the lamp's standard value. In the fifth experiment, the whole insertion loss in the range of 750–1650 nm changed at different measurement moments; this may be caused by a slight fluctuation of the Xe arc lamp.

There is no exact theory for the mechanism of the PB effect in bismuth-doped fibers, which is a complicated work because the exact structure of the BACs that emit NIR luminescence is still not known. There are three hypotheses about the NIR emission mechanism of BACs: (A) bismuth in higher valency, i.e.,  $\text{Bi}^{5+}$  and related molecules; (B) bismuth in lower valency, i.e., Bi,  $\text{BiO}$ ,  $\text{Bi}^+$ ,  $\text{Bi}^0$ , and cluster ions; and (C) point defects<sup>[21]</sup>. For the third hypothesis, Firstov proposed that the NIR emission model of BAC was a bismuth ion in proximity to an

oxygen-deficient center (ODC) (II) in bismuth-doped germanosilicate fibers (Bi-GSFs) in Ref. [22]. By comparing the photoinduced transmission spectra obtained under 532 nm pumping and 532 nm + 1555 nm dual wavelength pumping, Firstov *et al.* thought that bismuth ions did not participate directly in the PB process, and the PB effect was caused by the photoionization of ODC (II) forming BACs in Bi-GSF, which was a two-photon absorption process under 532 nm irradiation. Additionally, they thought that the PB effect was the same for BAC-Si and for BAC-Ge under 532 nm laser irradiation<sup>[23]</sup>. Ding *et al.* proposed that the PB effect was caused by the release of electrons of excited bismuth ion forming BAC-Si to the nearby defect ODC (II) in the BEDF<sup>[24]</sup>. They did comparative experiments on the BEDF pumped at 830, 980, and 1380 nm, and the results showed that BAC-Si had a PB effect under 830 and 1380 nm pumping, but not at 980 nm pumping, which indicated that excited bismuth ions were involved in the PB process of BAC-Si.

A study reported an energy transfer between BAC-Al and  $\text{Er}^{3+}$  in the BEDF under 830 or 980 nm pumping and indicated that the optical transition of BAC-Si was independent of other active centers<sup>[25]</sup>, so we did not consider the effect of  $\text{Er}^{3+}$  on PB of BAC-Si. Based on the literature review and our own experiments, the following mechanism is proposed to account for the PB. First, the ground state bismuth ions are pumped to the excited state under the 830 nm pumping. Second, some of them fall down to the metastable state via the nonradiative transition, while some release electrons to adjacent defects with the aid of thermal energy, resulting in the reduction of BAC absorption and luminescence. In addition, part of the bismuth ions on the metastable state level radiatively transit to the ground state, while the rest release electrons to adjacent defects, resulting in the PB. The whole process of PB is depicted in Fig. 5(a). D denotes bismuth ions forming the BAC-Si with a valence state of  $+x$ . The symbols \* and \*\* denote the first and second excited levels, respectively.  $\text{D}^*$  denotes bismuth ions with a valence state of  $+(x+1)$ . A denotes the point defect ODC (II). A- denotes the ODC (II) trapping an electron from bismuth.

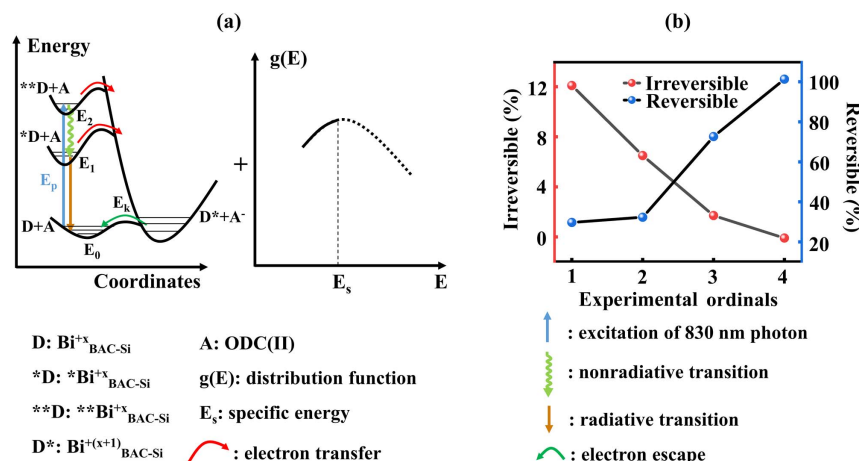


Fig. 5. (a) Photobleaching process and recovery relaxation using an electron transferring theory and distribution function concept of activation energy; (b) irreversible and reversible PB percentages after 73 h of recovery relaxation under repeated pumping.

$E_p$  and  $E_k$  are the photon excitation and thermal energy, respectively. On the basis of the above views, the concept of distribution function of activation energies  $g(E)$ <sup>[26,27]</sup> was introduced to illustrate the influence of repeated pumping and recovery relaxation process on PB. There is a distribution of the BACs' characteristic energies due to the irregularity of the glass structure<sup>[28]</sup>, so the activation energies of  $D^* + A$  and  $D + A$  transforming into the  $D^* + A$  have a distribution function of  $g(E)$ , which is the ratio of the number of BAC-Si with an activation energy  $E$  to the total number of BAC-Si, in our understanding. Similarly, the recovery relaxation process of  $D^* + A$  transforming into  $D + A$  also has a function of  $g(E)$ . With the aid of  $E_k$ , some BAC-Si are bleached, whose activation energies are less than or equal to  $E_s$  as shown by the solid line of  $g(E)$  in Fig. 5(a), while the rest of BAC-Si are stable; their activation energies are above  $E_s$ . This can explain the phenomenon that low temperature suppresses the PB effect of BAC-Si<sup>[29]</sup>. During the recovery relaxation process, part of the deactivated BAC-Si restores to the active BAC-Si at room temperature according to  $g(E)$ . Both the process of PB and recovery relaxation have  $g(E)$ s that may be the same or different in these processes. Thus, we can explain that the PB effect decreased and tended to be stable under repeated pumping conditions. Figure 5(b) shows the irreversible and reversible PB percentages after 73 h of recovery relaxation. The result indicated that the amount of irreversible PB gradually decreased under repeated pumping, while the amount of reversible PB increased and finally recovered fully. Based on the results and analysis above, the PB process of BAC-Si in the BEDF was further demonstrated.

#### 4. Conclusion

In this work, the PB effect of BAC-Si in the BEDF under repeated 830 nm laser pumping was studied. The results demonstrated that repeated pumping and recovery relaxation could stabilize the amount of BAC-Si that emitted NIR luminescence centering at ~1424 nm in the BEDF. We combined the electron transfer theory and the concept of distribution function of activation energies to further illustrate the PB process and the mechanism. Furthermore, based on this approach, a standard for evaluating the NIR emission stability of the BEDF can be established, which is essential for the long-time application of devices-based BEDF. In future work, we will further calculate the distribution function of activation energies  $g(E)$  of PB for BAC-Si in the BEDF. Moreover, the direction of our efforts will be to effectively regulate the valence state of bismuth and its surrounding coordination field in the fiber preforms phase, so as to effectively stabilize the luminescence stability of BACs in BDFs or BEDFs.

#### Acknowledgements

This work was supported by the Youth Program of the National Natural Science Foundation of China (No. 62105078), the Distinguished Young Scholars of the Natural Science

Foundation of Heilongjiang (No. JQ2022F001), the Youth Program of the Natural Science Foundation of Shandong (No. ZR2021QF009), the Young Elite Scientists Sponsorship Program by CAST (No. 2022QNRC001), the Fundamental Research Funds for the Central Universities (No. 3072021CFT2511), and 111 Project (No. B13015) to the Harbin Engineering University.

#### References

1. Y. Fujimoto and M. Nakatsuka, "Infrared luminescence from bismuth-doped silica glass," *Jpn. J. Appl. Phys.* **40**, L279 (2001).
2. L. Zhang, G. Dong, J. Wu, *et al.*, "Excitation wavelength-dependent near-infrared luminescence from Bi-doped silica glass," *J. Alloys Compd.* **531**, 10 (2012).
3. M. Peng, J. Qiu, D. Chen, *et al.*, "Bismuth- and aluminum-codoped germanium oxide glasses for super-broadband optical amplification," *Opt. Lett.* **29**, 1998 (2004).
4. N. Zhang, J. Qiu, G. Dong, *et al.*, "Broadband tunable near-infrared emission of Bi-doped composite germanosilicate glasses," *J. Mater. Chem.* **22**, 3154 (2012).
5. L. Wang, L. Tan, Y. Yue, *et al.*, "Efficient enhancement of bismuth NIR luminescence by aluminum and its mechanism in bismuth-doped germanate laser glass," *J. Am. Ceram. Soc.* **99**, 2071 (2016).
6. Q. Guo, B. Xu, D. Tan, *et al.*, "Regulation of structure rigidity for improvement of the thermal stability of near-infrared luminescence in Bi-doped borate glasses," *Opt. Express* **21**, 27835 (2013).
7. X. Meng, J. Qiu, M. Peng, *et al.*, "Infrared broadband emission of bismuth-doped barium-aluminum-borate glasses," *Opt. Express* **13**, 1628 (2005).
8. Y. Chu, Q. Hu, Y. Zhang, *et al.*, "Topological engineering of photoluminescence properties of bismuth- or erbium-doped phosphosilicate glass of arbitrary P2O5 to SiO2 ratio," *Adv. Opt. Mater.* **6**, 1800024 (2018).
9. E. M. Dianov, V. V. Dvoyrin, V. M. Mashinsky, *et al.*, "CW bismuth fibre laser," *Quantum Electron.* **35**, 1083 (2005).
10. Y. Luo, J. Wen, J. Zhang, *et al.*, "Bismuth and erbium codoped optical fiber with ultrabroadband luminescence across O-, E-, S-, C-, and L-bands," *Opt. Lett.* **37**, 3447 (2012).
11. J. Zhang, Z. M. Sathi, Y. Luo, *et al.*, "Toward an ultra-broadband emission source based on the bismuth and erbium co-doped optical fiber and a single 830nm laser diode pump," *Opt. Express* **21**, 7786 (2013).
12. S. V. Firstov, V. F. Khopin, I. A. Bufetov, *et al.*, "Combined excitation-emission spectroscopy of bismuth active centers in optical fibers," *Opt. Express* **19**, 19551 (2011).
13. Y. Chu, X. Fu, Y. Luo, *et al.*, "Additive manufacturing fiber preforms for structured silica fibers with bismuth and erbium dopants," *Light Adv. Manuf.* **3**, 358 (2022).
14. Q. Zhao, Y. Luo, Y. Tian, *et al.*, "Pump wavelength dependence and thermal effect of photobleaching of BAC-Al in bismuth/erbium codoped aluminosilicate fibers," *Opt. Lett.* **43**, 4739 (2018).
15. B. Zhang, Y. Luo, M. Ding, *et al.*, "Thermally aggravated photo-bleaching of BAC-Al in bismuth/erbium co-doped optical fiber," *Opt. Lett.* **44**, 4829 (2019).
16. S. Wei, Y. Luo, D. Fan, *et al.*, "BAC activation by thermal quenching in bismuth/erbium codoped fiber," *Opt. Lett.* **44**, 1872 (2019).
17. B. Zhang, S. Wei, M. T. A. Khan, *et al.*, "Dynamics study of thermal activation of BAC-Si in bismuth/erbium-codoped optical fiber," *Opt. Lett.* **45**, 571 (2020).
18. M. Ding, S. Wei, Y. Luo, *et al.*, "Reversible photo-bleaching effect in a bismuth/erbium co-doped optical fiber under 830 nm irradiation," *Opt. Lett.* **41**, 4688 (2016).
19. H. Xu, B. Yan, Y. Luo, *et al.*, "Pump-induced photobleaching and thermal dependent recovery of BAC-Si in Bi/Er co-doped optical fiber by 830 nm laser irradiation," *Opt. Commun.* **476**, 126319 (2020).
20. J. Hao, Y. Chu, Z. Ma, *et al.*, "Effects of thermal treatment on photoluminescence properties of bismuth/erbium co-doped optical fibers," *Opt. Fiber Technol.* **46**, 141 (2018).

21. M. Peng, G. Dong, L. Wondraczek, *et al.*, "Discussion on the origin of NIR emission from Bi-doped materials," *J. Non-Cryst. Solids* **357**, 2241 (2011).
22. S. Firstov, S. Alyshev, M. Melkumov, *et al.*, "Bismuth-doped optical fibers and fiber lasers for a spectral region of 1600–1800 nm," *Opt. Lett.* **39**, 6927 (2014).
23. S. Firstov, S. Alyshev, V. Khopin, *et al.*, "Photobleaching effect in bismuth-doped germanosilicate fibers," *Opt. Express* **23**, 19226 (2015).
24. M. Ding, J. Fang, Y. Luo, *et al.*, "Photo-bleaching mechanism of the BAC-Si in bismuth/erbium co-doped optical fibers," *Opt. Lett.* **42**, 5222 (2017).
25. Q. Zhang, J. Zhang, Y. Luo, *et al.*, "Energy transfer enhanced near-infrared spectral performance in bismuth/erbium codoped aluminosilicate fibers for broadband application," *Opt. Express* **26**, 17889 (2018).
26. A. Kharakhordin, S. Alyshev, E. Firstova, *et al.*, "Analysis of thermally activated process in bismuth-doped GeO<sub>2</sub>-SiO<sub>2</sub> glass fibers using the demarcation energy concept," *Opt. Mater. Express* **9**, 4239 (2019).
27. B. Poumellec, "Links between writing and erasure (or stability) of Bragg gratings in disordered media," *J. Non-Cryst. Solids* **239**, 108 (1998).
28. S. Alyshev, A. Kharakhordin, E. Firstova, *et al.*, "Photostability of laser-active centers in bismuth-doped GeO<sub>2</sub>-SiO<sub>2</sub> glass fibers under pumping at 1550 nm," *Opt. Express* **27**, 31542 (2019).
29. M. Ding, Y. Luo, J. Wen, *et al.*, "Dynamic behavior of pumping radiation induced photo-bleaching effect on BAC-Si in bismuth/erbium co-doped optical fibers," *Proc. SPIE* **10512**, 1051226 (2018).